Nitration of Jharia Basin Coals, India: a study of structural modifications by XRD and FTIR Techniques

Prabal Boral
Central Institute of Mining and Fuel Research CSIR
Atul K. Varma
Indian School of Mines
Sudip Maity (sudip_maity@yahoo.com)
Central Institute of Mining and Fuel Research CSIR https://orcid.org/0000-0002-6507-2764

Research

Keywords: Coal, Micro-Structure, Nitration, XRD, FT-IR

Posted Date: August 18th, 2020

DOI: https://doi.org/10.21203/rs.3.rs-60892/v1

Version of Record: A version of this preprint was published at International Journal of Coal Science & Technology on April 8th, 2021. See the published version at https://doi.org/10.1007/s40789-021-00422-8.

Abstract

Four coal samples from Jharia basin, India are treated with nitric acid in glacial acetic acid and aqueous media to find out the chemical, petrographic and spatial structure of the organic mass by X-ray diffraction and FT-IR techniques.

X-ray parameters of coal like interlayer spacing (d_{002}), crystallite size (L_c), aroamticity (f_a), average number of aromatic layers (N_c), and coal rank (I_{26}/I_{20}) have been determined using profile-fitting software. Considerable variation is observed in treated coals in comparison to the demineralized coals. The d_{002} values of treated coals have increased in both the media showing increase in disordering of organic moieties. A linear relationship has been observed between d_{002} values with the volatile matter of the coals. Similarly, the d_{002} values show linear relationship with C_{dmf}contents for demineralized as well as for the treated coals in both the media. The *Lc* and *Nc* values have decreased in treated coals corresponding to demineralized coals. The present study shows that nitration in both the media is capable of removing the aliphatic side chains from the coals and aromaticity (f_a) increases with increase in rank and shows a linear relationship with the vitrinite reflectance. The corresponding I_{26}/I_{20} values are least for treated coals in glacial acetic acid medium followed by raw and then to treated coals in aqueous medium.

FT-IR studies show that coal arenes of the raw coals are converted into nitro-arenes in structurally modified coals (SMCs) in both the media, the corresponding bands at 1550 – 1490 cm^{-1} and 1355 – 1315 cm^{-1} respectively. FT-IR study confirms that nitration is the predominant phenomenon, though, oxidation and nitration phenomena takes place simultaneously during treatment with nitric acid to form SMCs. In comparison to raw coals, the SMCs show higher aromaticity and may be easily converted to coal derived products like activated carbon and specialty carbon materials.

1.0 Introduction

Coal has manifold uses, as for instance, solid fuel, gives coke for metallurgical use, coal chemicals and many more. Several chemical products can be produced from the coal and/or its by-products. Coal has several advantages when considered as a feedstock for aromatic chemicals and carbon based materials. It can be used in producing activated carbon (AC), carbon molecular sieve (CMS), specialty carbon materials (viz.: fullerene, artificial graphite, artificial diamond), composites of coal with other polymers, humic acid preparations etc.

Hence, the study molecular structure of coals and their structurally modified counter parts are very much essential to understand their basic nature and for suitability towards more meaningful industrial utilization. Coal is essentially a very heterogeneous and complex material and many a models have been proposed to understand the molecular structure of it and their structurally modified counterparts (Domazetis and James 2006; Mathews and Chaffee 2012; Li et al. 2015). Earlier, Hirsch (1954) carried out X-ray diffraction studies of low rank coals and anthracite. He found that the low rank coals up to carbon content 85% have “open structure”. Many studies like TEM/SEM, XRD, FTIR, Raman Spectroscopy, NMR and HR-TEM have been performed for coal molecular structure determination (Solum et al. 1989; Dangyu et al. 2011; Baysal et al. 2016; Barbara et al. 2019).

The role of X-ray diffraction is very important in coal science. Powder diffraction technique can be used to study the different phases present in coal. To address the heterogeneity of coal, this technique has immensely important as it uses relatively large amount of the sample and collects most of the intensities scattered from the sample (Lu et al. 2001). Coal has an intermediate structure between graphite and amorphous carbon, so-called turbostratic structure or random layer lattice structure (Maity and Mukherjee 2006). It also contains significant amount of highly disordered material, amorphous carbon, which is responsible for the background intensity of the diffractograms. However, recent development of computer techniques has enabled more accurate calculations and detailed analysis of XRD profiles. Wertz's group (1994–2000) has made extensive studies of coals using XRD technique and quantitatively characterized both mineral matter and organic matrix of coals. XRD analysis is a fundamental method for evaluating carbon stacking structure. The degree of graphitization, the interlayer spacing (d_{002}), and the crystallite size (L_c), aromaticity (f_a), average number of aromatic layers (N_C) and XRD rank parameter (I_{26}/I_{20}) have been established as the parameters for evaluating structure of highly crystalline carbon materials (Boral et al. 2015).

Fourier Transform Infrared (FTIR) spectroscopy exploits the fact that molecules absorb or transmit specific frequencies that are characteristic of their structure. FTIR spectrum of coal is generally studied in mid-infrared zone, approximately 4000–400 cm^{-1} wave number range. Infrared spectroscopy gives information on the vibrational and rotational modes of motion of a molecule and hence an important technique for identification and characterization of functional groups. The Infrared spectrum of an organic compound provides a unique fingerprint, which is readily distinguished from the transmission patterns of all other compounds. Fourier transform is used to process the data from interferometer instrument. Modern FTIR instrument uses a laser-light, powerful computer and advanced software. The software performs processing, manipulation, plotting, resolution enhancement, peak position, area measurement, library searching (Painter et al. 1978; Painter and Colemon 1979; Solomon et al. 1990; Tamarkina et al. 2002). Radial distribution function (RDF) obtained from Fourier Transformation of molecular scattering is used to examine the molecular level structuring of coal. Tamarkina et al. 2002 used FTIR to study modification of different rank coals in equimolar nitric acid and acetic anhydride mixture.

To study the structural variations, four samples have been collected from Jharia Basin of India. Jharia Basin coal is very important as it is the only caking/coking coal producing horizon of India. The coal bearing horizon of the basin is subdivided into two stratigraphic formations, viz., Barakar and Raniganj. The Barakar Formation coals are the only source of the prime coking coal of India, while the Raniganj measure coals are the high volatile medium coking coals. For all the coal seams, it is observed that their maturity gradually decrease from west towards east, in both the coal measures. Coals of the Barakar Formation are generally low in moisture (0.5 to 2.0%) and medium to low volatile caking coal. The coals of the Raniganj Formation contain slightly higher moisture and high volatile matter content than the coals of Barakar Formation. All the samples were demineralized using standard HCl + HF method to avoid the effect of mineral matter in instrumental analyses (Maity and Mukherjee 2006). Each of the demineralized coal samples have been modified using nitric acid treatment in glacial acetic acid and in aqueous medium (Maity and Choudhury 2008). Thus, twelve numbers of samples have been prepared in total for the present study.

2.0 Experimental

2.1 Collection of Sample

Jharia basin forms a part of the Damodar valley basins which include Jharia, Raniganj, Bokaro, Karanpura and Ramgarh coalfields. These coalfields are separated from each other by Precambrian rocks in the outcrops. Jharia Coalfield (JCF) is situated about 260 km northwest of Kolkata in the heart of Damodar valley mainly along the north of the Damodor river. The coalfield is bounded between latitude N23º37'– N23 º 52' and longitudes E86º06' – E86º36'and lies within the district of Dhanbad. This sickle shaped coal basin extends for about 38 km in an east-west direction and a maximum of 19 km in north-south direction and covers an area of about 456 sq. km. Out of this area; Barakar formation occupies an area of 216 sq. km., Raniganj Formation 54 sq. km. and rest Barren Measures 180 sq.km (Krishnan, 1982).

The general stratigraphic succession (Chandra 1992) of the area is that the basement of metamorphic rocks overlain by the Talchir Formation followed by the Barakar Formation, which is the main coal bearing horizon. Above it, comes the Barren Measures (devoid of coal), which is followed by the coal-bearing Raniganj Formation. The Raniganj Formation is the uppermost coal bearing Formation in the Jharia coalfield. The Barakar Formation having a total thickness of about 800-1250m contains about 25 coal horizons out of which 18 are regionally persistent. The upper coal measures of Raniganj Formation have a thickness around 800 m and contain 12 coal horizons of which 4 to 5 are persistent in nature. In both the formations the persistent coal seams have been numbered from bottom.

The present study is carried out by collecting samples from of Mohuda (MH), Gasalitand (GT), Salanpur (SL) and Shatabdi (ST) mines of Jharia Coalfield forms a part of the Damodar Valley basin. The details of coal samples used for the present study are shown in Table 1.

Table 1
Details of the collected samples:

S. No.	SN	Seam	Mine	Formation	Basin	Age
1	MH	R-III (Top)	Mohuda	Raniganj	Jharia	Late Permian
2	GT	XII/XIII	Gasalitand	Barakar	Jharia	Early Permian
3	SL	III	Salanpur	Barakar	Jharia	Early Permian
4	ST	II	Shatabdi	Barakar	Jharia	Early Permian

The collected samples were prepared for the study of chemical and structural parameters in the sample sizes crushed to below 212 μ (IS 436 Part 1/Sec 1 2001), while samples for petrographic analysis were prepared by passing through 1 mm sieve (controlled crushing) following standard procedures (IS 9127 Part 2 2002). The GCV of each sample was measured using Automatic Bomb calorimeter (Model AC-350 isoperibol bomb calorimeter, Leco, USA) following standard (ASTM D5865 2013) procedure. The ultimate analysis of coal involves determination of the elemental composition of coal. It is expressed in terms of weight percentages of carbon (C), hydrogen (H), nitrogen (N), sulphur (S), and oxygen (O). Percentages of elemental C, H, N and S were determined while O was obtained by difference from hundred percent. Information derived from ultimate analysis is used for selection of coal for various efficient utilization purposes. The Leco (USA) make CHN-1000 analyzer was used for determination of carbon, hydrogen and nitrogen percentages of each of the air-dried

samples following standard (ASTM D5373 2016) procedure. For sulphur determination of the samples, Leco (USA) make SC-132 was used following standard (ASTM D5016 2016) procedure, which is a microprocessor-based instrument, and has a control console for each system and a measurement unit with a built-in-balance.

The maceral analyses and vitrinite reflectance of each sample were carried out in micro-petrographic analysis of coal. The maceral analysis was carried out following standard (IS 9127 Part 3 2002) procedure. Reflectance measurement is carried out following standard (IS 9127 Part 5 2004) procedure.

Reflected light polarized microscopes (Make: Leitz; Model: MPV Compact, Germany and Make: Leica, Model: DMRX P HC, Germany) have been used to study the maceral composition and reflectance measurements of the samples.

2.2 Demineralization of samples

All the raw coal samples contain inorganic mineral matter. The intensity of the diffraction peaks of these inorganic minerals is much sharper and stronger than that of the broad humps of the organic matter present in coal. It is very difficult to obtain accurate crystalline peaks of organic matters in X-ray diffraction pattern of crystalline organic matters in presence of inorganic mineral matters. So, the mineral matters present in coal are removed by demineralizing the coal samples using standard HCl + HF solution to alleviate this problem (Maity and Mukherjee, 2006).

Each ten grams of air dried sample of 212 μ (X 72 mesh) size was accurately weighed and transferred to a Teflon beaker. To this 60 ml of concentrated HCl of 36.5 wt % was added slowly keeping it in a water bath. The temperature of the water bath is kept at 60 ºC. The mixture is stirred vigorously by a Teflon rod for three hours. Then the coal was filtered and washed with hot distilled water to remove HCl. The filtered HCl-treated coal was again treated with 60 mL concentrated HF solution of 48 wt% purity. The mixture was again kept in water bath of 60 ºC and stirred for another three hours. Finally, the HF treated coal was filtered and washed with hot distilled water to remove HF from coal. Removal of acid from coal is confirmed by pH test of the samples. Then residual coal in the filter paper is dried in an air-oven for 5–6 hours at 50 $^{\circ}$C. The Demineralization was confirmed by the weight loss of the coal samples to at least less than 2% effective mineral matter for the samples.

2.3 Chemical modification procedures

Structural modification was carried by oxidative pretreatment of coal. Two types of chemical treatments were carried out for each of the demineralized coal samples to make structurally modified coals (SMCs). The demineralized coal samples were treated with concentrated nitric acid in different media viz. in glacial acetic acid and in aqueous media to form SMCs (Maity and Choudhury 2008).

2 g of demineralized coal was weighed accurately and 10 mL of glacial acetic acid was mixed thoroughly in beaker. The mixture was kept in a water bath at a temperature of 15–20 ºC by adding ice to the water bath. The temperature of the bath was monitored so as to maintain the desired temperature. To this mixture, 3 mL of concentrated nitric acid (HNO_3 at 68 wt %) was added drop by drop and stirred thoroughly. This 3 mL HNO_3 was mixed to the mixture of coal and glacial acetic for at least half an hour duration and after that kept for 24 h. After 24 h, the mixture is diluted with 250 mL/g distilled water and left for another 24 h. The mixture was then filtered and washed with hot distilled water till neutralization (pH ~ 7.0) was attained. Then the treated coal was

dried in an air-oven at 50 ºC for 5–6 h and kept in desiccators. After treatment of each sample the difference in weight was measured.

In the second treatment, two grams of demineralized coal was taken in a refluxing condenser. Pure nitrogen gas was passed through it before the treatment for purging. Then 60 mL of 30% nitric acid was mixed to the coal. The coal acid mixture was heated at 105 ± 5 ºC and stirred well. The reaction continues for 8–10 h or till the end of any gas evolution from the coal-acid mixture. The residue left in the flask was filtered and washed with hot distilled water till any trace of nitric acid is removed. The neutralization was confirmed by pH test. After each treatment, the sample was dried in an air-oven at 50 ºC for 5–6 h and kept in desiccators and the difference in weight is calculated using the formula:

$$\Delta\ wt\% = (W_f - W_i)/W_i$$

Where, W_f and W_i are the final and initial weight of the coal sample after and before treatment of coal respectively.

The demineralized coal samples were coded with suffix (D), nitric acid treated coals in glacial acetic acid medium with suffix (G) and aqueous nitric acid treated coals with (A). As for example the Mohuda demineralized coal (MH_D), viz. (MH_G) for Mohuda nitric acid treated coals in glacial acetic acid medium and (MH_A) for aqueous nitric acid treated coals.

2.4 X-ray diffraction analysis

X-ray Diffraction (XRD) analysis was performed by using a D-8 ADVANCE (Bruker AXS, Germany) X-ray Diffractometer. This was used to collect the X-ray intensities of the demineralized and treated coals in the 2θ range of 10–90° with Bragg-Brentano geometry, using parallel beam Cu K_α (40 kV, 40 mA) radiation. An X-ray amorphous sample holder was used for coal sample loading, and the scan was made in locked couple step scan mode (0.02°/step), with 2 s at each step.TOPAS 3.0 from Bruker AXS (2005), Germany was used for de-convolution of the diffractograms in the 2θ region of 10–35°. Two symmetrical Gaussian peaks were fitted for determination of π-band and γ-band to determine the d_{002} and position of γ-band (D_γ) respectively. XRD profile curve fitting of two Gaussian peaks for the Mohuda (MH) demineralized coal in the range of 10–35° is shown in Fig. 1 as an example. The carbon-related peaks around 20–26°can be categorized into π (002-band) and γ-band for aromatic and aliphatic chains respectively. The π-band due to aromatic ring stacking occurs near 26°, while γ-band around 20°, are believed to be derived from aliphatic chains. TOPAS 3.0 software was used for refinement of π-band and γ-band to determine the d_{002}, position of γ-band (D_γ), average crystallite size (L_c), average number of aromatic layers (N_c), ratio of intensity of π-band and γ-band (I_{26}/I_{20}) and aromaticity (f_a) (Maity and Mukherjee 2006; Boral et al. 2015). The software package uses the fundamental parameter approach (FPA) and is therefore capable of estimating the instrumental influence. The Double-Voigt approach in TOPAS is used with both calculated FPA and measured instrument functions. XRD analyses were carried out for all the demineralized coal samples and their corresponding SMCs formed by nitration in glacial acetic acid medium and aqueous medium.

2.5 Fourier Transform Infra Red Spectroscopy

Fourier transform infra red spectroscopy (FTIR) is extensively used for quantitative as well as for qualitative analysis in almost all fields of science (Painter et al. 1978; Painter and Colemon 1979; Solomon et al. 1990). Bruker (Germany) make 3000 Hyperion Microscope with Vertex 80 model FTIR-imaging system has been used to analyze the samples.

The FTIR spectra of all the samples were carried out in the range of spectral band of 4000 to 450 cm^{-1}. For each sample analysis, thirty two scans are co added at a resolution of 2 cm^{-1}. For spectral analysis, KBr matrix method was applied to prepare the samples. Sample and dry KBr in the ratio of 1:100 are ground and mixed in an agate mortar. Pellets of 13 mm diameter are prepared using 250 mg of this mixture by pressing it in an evacuated die at 10 tonnes pressure in a hydraulic press. Origin 6.1 software was used to de-convolute FTIR spectrum and multi-peak Gaussian probability density function fit obtained for each functional group. Multi-peak Gaussian probability curve fit of FTIR analysis of Mohuda (MH) coal is shown as an example in Fig. 2. The area under each functional group was calculated for demineralized as well as treated coals in glacial acetic acid and in aqueous nitric acid by using the software.

3.0 Results And Discussions

3.1 Coal Properties

Proximate, Ultimate, Gross Calorific Value (GCV) and Petrographic analyses data of the raw coals are shown in Table 2. The VM_{dmf} contents show that (MH, GT and SL) belong to medium volatile coals (25.8 – 30.3 %), while ST having 21.0 wt % VM yield belongs to low volatile coal. Fixed carbon (FC_{dmf}) ranged between 69.7 – 79.0 % and GCV_{dmf} of the samples vary between 8450 – 8640 kcal/kg and are of high maturity.

Petrographic analyses of coals reveal vitrinite reflectance (VR_r) 0.85 – 1.24 % (Table 2). Mineral free vitrinite content varies between 70.8 and 37.9 %, liptinite 0.4 and 4.6 % and inertinite between 37.9 and 70.8 %. The volatile matter yield is the combined effect of maceral contents of the coals (Borrego et al. 2000; Guerrero and Borrego 2013). It is considered to be the highest for liptinite maceral followed by vitrinite and inertinite. It can be seen from the analyses that liptinite content of the samples are not very significant. Hence a plot between vitrinite content and volatile matter was drawn (Fig. 3) which shows a straight line curve with R^2 value of 0.87. Also, the VM is considered as the function of hydrogen and hydrogen content decreases with decrease in VM (Table 2).

SN	VM_{dmf}	FC_{dmf}	GCV_{dmf}	C_{dmf}	H_{dmf}	S_{dmf}	N_{dmf}	O_{dmf}	V_{mmf}	L_{mmf}	I_{mmf}	VR_r%
	wt %	wt %	kcal/kg	wt %	wt %	wt %	wt %	wt %	Volume %			
	Dry mineral free basis								Mineral matter free basis			
MH	30.3	69.7	8550	86.46	5.87	0.47	1.91	5.30	70.8	4.6	24.6	0.85
GT	28.1	71.9	8630	87.37	5.44	0.65	1.71	4.82	63.7	0.4	35.9	1.05
SL	25.8	74.2	8640	89.02	5.23	0.80	1.98	2.97	43.9	0.9	55.2	1.17
ST	21.0	79.0	8450	90.88	5.19	0.64	1.82	1.82	37.9	2.9	59.2	1.24

Table 2: Proximate, Ultimate, Gross Calorific value and Petrographic analyses of coals

Explanations: SN= sample name, VM= volatile matter yield, FC= fixed carbon, GCV= gross calorific value, C=carbon, H=hydrogen, S=sulphur, N=nitrogen, O=oxygen, $_{dmf}$= dry mineral free V=vitrinite, L=liptinite, I=inertinite, MM= mineral matter, VR_r = mean random reflectance of vitrinite, $_{mmf}$= mineral matter free basis.

Fig. 3: Relation of Vitrinite content with respect to Volatile Matter.

3.2 Changes in weight on nitration

The change in weight due to treatment is shown in Table 3. It is observed that in glacial acetic acid medium, the weights of the samples have increased. Since, the medium is non-aqueous; less oxidation has taken place in the coal moieties resulting into gain in weight of all the studied samples. MH coal shows reduction in weight (shown with negative sign in the Table 3) in the case of nitration in aqueous medium. Rest of the samples treated with aqueous nitric acid has gained weight. MH being low in rank (VRr = 0.85 %) in comparison to the other three samples, oxidation is predominant phenomenon with simultaneous nitration in aqueous medium which has removed the aliphatic side chains resulting into decrease in weight of the said samples. Nitration is the predominant phenomena with simultaneous oxidation in stronger aqueous medium for higher rank coals.

Sl. No.	SN	G. Ac. Acid+HNO_3	Aq.HNO_3
		Change in wt %	Change in wt %
1	MH_D	19.08	-10.39
2	GT_D	19.78	13.59
3	SL_D	15.29	15.00
4	ST_D	16.37	15.44

Table 3: Change in weight due to nitration

Fig. 4: Relation of d_{002} with respect to Volatile Matter.

3.3 X-ray Diffraction studies

The results of X-ray scattering analysis are shown in Table 4. The d_{002} values of demineralized coals [d_{002} Å (D)] are plotted against VM_{dmf} wt% (Table 2) and shown in Fig. 4. It is observed that d_{002} decreases with decrease in VM_{dmf} wt% and maintains a linear relationship with coefficient of determination, R^2=0.82. It is known that d_{002} decreases with increase in maturity, vis-à-vis decrease in volatile matter yield of the coal (Lu et al. 2001).

It is found that the corresponding inter layer spacing of π- band (d_{002}) are the least for raw coals followed by d_{002} values of treated coals in aqueous medium and then to glacial acetic acid medium (Table 4). The d_{002} values of demineralized coals as well as treated coals are plotted against dry mineral free carbon of coal samples (C_{dmf}) which is shown in Fig. 5.a – 5c and it is observed that d_{002} value decreases with the increase of C_{dmf}. A similar relationship was found between $d_{002}$and elemental carbon (Maity and Mukherjee 2006; Sonibare et al. 2010, Manoj and Kunjonama 2012) for demineralized coals where a linear relationship between d_{002} and elemental C_{dmf} was established. The nature of the graphs is similar for the demineralized as well as treated coals. An inverse relationship is found between C_{dmf} and d_{002} (D), with increase in C_{dmf} content d_{002} decreases with R^2= 0.88 (Fig. 5a). Similar trend is also observed for the chemically modified coals having R^2= 0.93 and R^2= 0.94 for d_{002} (G) and d_{002} (A) respectively (Fig. 5b & 5c).

S N	d_{002} (Å)	L_c(Å)	f_a	N_c	I_{26}/I_{20}	$D\gamma$(Å)
MH_D	3.484	23	0.44	6.60	1.82	4.30
MH_G	3.487	21	0.47	6.02	1.56	4.14
MH_A	3.486	21	0.68	6.02	2.90	4.20
GT_D	3.471	25	0.50	7.20	1.97	4.27
GT_G	3.480	21	0.51	6.03	1.75	4.26
GT_A	3.473	22	0.71	6.33	2.95	4.31
SL_D	3.454	25	0.52	7.24	2.20	4.19
SL_G	3.466	23	0.53	6.64	1.85	4.18
SL_A	3.460	23	0.72	6.65	3.09	4.12
ST_D	3.451	25	0.53	7.24	2.54	4.03
ST_G	3.462	24	0.54	6.93	2.21	4.28
ST_A	3.452	24	0.73	6.95	3.38	4.07

Table 4: XRD analysis of demineralized and nitric acid treated coals

It is found that the corresponding d_{002} values of coals treated with nitric acid in glacial acetic acid and aqueous media are increased. Aqueous medium being stronger in the present studied mediums might have dissolved the more aliphatic content of coal resulting in relative increase of aromatic moieties which lead to decrease in inter layer spacing (d_{002}) in comparison to nitration in glacial acetic acid medium.

The results of mean crystallite size (L_c) of demineralized coals and their SMCs formed due to nitration in glacial acetic acid medium and in aqueous medium are shown in Table 4. The L_c values of demineralized coals increase with increase in carbon content and vitrinite reflectance indicating crystallite sizes increase with increase in rank of the coals (Table 2 & 4). Due to nitration, the disordering of molecular structure has taken place leading to decrease in mean crystallite size (L_c) of SMCs in comparison to the demineralized coals. Similar studies were carried out by several other workers (Sonibare et al. 2010; Manoj and Kunjonama 2012) and corroborates with the present study.

The variation of aromaticity (f_a) of demineralized as well as nitric acid treated coal in glacial acetic acid medium and aqueous medium are shown in Table 4. It is found that corresponding f_a values are least for demineralized coals followed by treated coals in glacial acetic acid medium and then to aqueous medium. The increase in aromaticity in aqueous nitric acid treated coals is much more than that of nitration in glacial acetic acid medium. This suggests that aqueous medium is stronger than that of glacial acetic acid medium and is capable of removing more aliphatic contents resulting in more increase in aromaticity. The change in weight in both the media also indicates towards a similar conclusion (Table 3). The aliphatic contents are easily removed by aqueous nitric acid resulting into decrease in weight for MH coal and for relatively higher rank coals also the increase in weight is less in comparison to nitric acid treated coals in glacial acetic acid medium.

The vitrinite reflectance (*VRr*) is also plotted against f_a and shown in Fig. 6a – 6c. It shows an almost straight line relationship with coefficient of determination of R^2=0.96 for demineralized coals, R^2=0.9958 for treated coals in glacial acetic acid and R^2 = 0.998 for coals with nitration in aqueous medium. It is to mention here that vitrinite reflectance is a very good indicator of rank and suggests that the aromaticity is more dependent on rank of the coals. The significant finding of this study is that nitration in the aromatic structure of coals is the predominant phenomenon with simultaneous oxy-destruction of aliphatic side chains resulting increase in the aromaticity. It also shows that aqueous medium being stronger between two media used for formation of SMCs of present study is capable of removing more aliphatic components resulting into more aromaticity of the samples in the said medium.

The average number of aromatic layers (N_c) for demineralized and the treated coals are shown in Table 4. It can be observed that N_c have increased with increase in C_{dmf} content (Table 2). Similar kind of relationship between N_c and C_{dmf} has also been observed for demineralized pyrolyzed coals (Takagi et al. 2004) as observed in the present work. Also, the N_c values are maximum for demineralized samples followed by the corresponding nitric acid treated coals in aqueous medium and then to glacial acetic acid medium. This suggests that in treated coals, the structure of the coals is disordered due to nitration which reduced the average aromatic layers of SMCs. The degree of disorder is more in the case of glacial acetic acid treated coals than in aqueous medium.

The results of intensity ratio of π- and γ- band (I_{26}/I_{20}) is also known as X-ray rank parameter and for demineralized and treated coals in both the media are shown in Table 4. The variation of I_{26}/I_{20} values of raw

as well as treated coals are plotted against C_{dmf}content and shown in Fig. 7.a – 7c. The nature of curves is similar for raw as well as treated coals in both the nitration media. A very good linear fit of the curves are observed having R^2=0.9963 for demineralized coal (Fig 7a). The nitric acid treated coals show linear increase of R^2 = 0.96 in glacial acetic acid medium and aqueous medium respectively (Fig. 7b and Fig. 7c). Thus, the chemical (C_{dmf}) and X-ray (I_{26}/I20) rank parameters agree with each other to express the maturity of coal. Inter-layer spacing of γ-band (D_γ) occurs around 20° and is believed to be derived from aliphatic side chains of coal molecules. The Dγ values obtained for demineralized and SMCs formed do not show any trend in the present study (Table 4).

3.4 Fourier Transform Infrared Spectroscopy (FTIR)

The broad strong stretching band of –OH (hydroxyl) group is shown in the range of 3600 –3200 cm^{-1} produced mainly due to moisture in coal. In some of the samples stretch band of alkene (=CH_2) of small to medium intensity of (3100 – 3010cm^{-1}) are observed. The 2950 – 2800 cm^{-1} appeared as sharp peak of medium intensity and are assigned to aliphatic and alicyclic –CH_3, –CH_2 and –CH groups; though the major contributor is the –CH_2 groups. The peaks ~1700 cm^{-1} has appeared due to strong stretching band of carbonyl/ketone (C=O) group. The bending vibration of alkane (-CH_3) appears in the range of 1470 – 1350 cm^{-1}. The peaks ~1600 cm^{-1} are observed due to medium to stretching bands of C=C aromatic compounds. Ester and/or ether groups are formed at 1320 – 1210 cm^{-1}. The region between 900 – 700 cm^{-1} is assigned to various bands related to aromatic, out-of-plane C-H bending, –OH group with different degree of substitution.

In the samples of nitric acid treated coals, both in glacial acetic acid medium and aqueous medium, a distinct stretch asymmetric strong band of nitro (-NO_2) groups of aromatic compound appears in the range of 1550 – 1490 cm^{-1}. A –CH_3 bending band and –CH_2 group in bridges of variable intensity has been observed in the range of 1430 – 1290 cm^{-1}. It has also been observed that strong stretch symmetrical nitro (NO_2) group appears in the range of 1355 – 1315 cm^{-1} in nitric acid treated coals in both the media. Covalent nitro-groups (Ar–O–NO_2) are formed at 1255-1300 cm^{-1}. A strong stretch band of ether (C–O) appeared in 1300 – 1000 cm^{-1}. A deformation bending arene bond of nitro-groups is absent in the range of 860 – 840 cm^{-1}.

The FTIR curves of demineralized coals, nitration in glacial acetic medium and nitration in aqueous medium are suffixed by D, G and A respectively and shown in Fig. 8 to Fig. 11. The areas of functional groups for all the demineralized as well as nitric acid treated coals in both non-aqueous and aqueous medium have been calculated by Gaussian probability density function using Origin 6.1 software and shown in Table 5 – Table 8. In order to quantify the replacement of aliphatic side chains by nitro groups an attempt has been made to measure the area under peaks of aliphatic and alicyclic (-CH) functional group of vibration (2950 – 2800 cm^{-1}) and bending vibration of alkane (-CH; 1470 – 1350 cm^{-1}) are added for demineralized (raw) coals and corresponding nitric acid treated coals in both the media. The decrease in total areas of alkane group of raw and treated coals suggests the replacement of aliphatic side chains by nitro group. Total area of -CH_3 group is decreased from 13.72 cm^2 at 2917 cm^{-1}, 2853 cm^{-1} and at 1441 cm^{-1} for demineralized coal to 10.76 cm^2 at 2922 cm^{-1}, 2856 cm^{-1} and at 1449 cm^{-1} for MH_G coal (Table 5a & 5b). Total area decreased to 13.62 cm^2 of -CH_3 group in MH_A at 2924 cm^{-1}, 2853 cm^{-1} and at 1450 cm^{-1} coal (Table 5a & 5c).

MH_D					
Wave Number (cm^{-1})	Functional Group		Type of Vibration	Intensity	Area (cm^2)
3420	O-H	Phenolic/Hydroxyl	Stretch, H-bonded	Strong, broad	1.54
3043	=C-H	Alkene	Stretch	Strong	0.86
2917	C-H	Alkane	Stretch, symmetric	Strong	4.00
2853	C-H	Alkane	Stretch, asymmetric	Strong	3.01
1897	=C-H	Alkene	Stretch, asymmetric	Strong	0.48
1595	C=C	Arom./Arene	Scissoring	Med	16.66
1441	-C-H	Alkane	Bending	Variable	6.72
1368	N=O	Nitro	Stretch, symmetric	Strong	1.19
1215	C-O	Ether/Ester	Stretch	Strong	41.00
863	=C-H/ C=C/N-H	Alkene/Arene/Amine	Bending	Strong	1.42
811	=C-H/ C=C/N-H	Alkene/Arene/Amine	Bending	Strong	2.46
749	O-H/ C=C/N-H	Alcohol/Arene/Amine	Bending, out-of-plane	Weak	2.91

Table 5a

MH_G					
Wave Number (cm^{-1})	Functional Group		Type of Vibration	Intensity	Area (cm^2)
3423	O-H	Phenolic/Hydroxyl	Stretch, H-bonded	Strong, broad	16.46
3069	=C-H	Alkene	Stretch	Strong	0.44
2922	C-H	Alkane	Stretch, symmetric	Strong	6.03
2856	C-H	Alkane	Stretch, asymmetric	Strong	2.72
1926	=C-H	Alkene	Stretch, asymmetric	Strong	0.82
1713	C=O	Carbonyl/Ketone	Stretch	Strong	9.27
1608	C=C	Arom./Arene	Scissoring	Med	19.78
1531	N=O	Nitro Arene	Stretch, asymmetric	Strong	5.73
1449	-C-H	Alkane	Bending	Variable	2.01
1372	N=O	Nitro Arene	Stretch, symmetric	Strong	5.78
1333	N=O	Nitro Arene	Stretch, symmetric	Strong	65.14
1032	C-O	Ether/Ester	Stretch	Strong	2.56
892	=C-H/ C=C/N-H	Alkene/Arene/Amine	Bending	Strong	0.06
822	=C-H/ C=C/N-H	Alkene/Arene/Amine	Bending	Strong	0.54
753	O-H/ C=C/N-H	Alcohol/Arene/Amine	Bending, out-of-plane	Weak	1.11

Table 5b

MH_A					
Wave Number (cm^{-1})	Functional Group		Type of Vibration	Intensity	Area (cm^2)
3435	O-H	Phenolic/Hydroxyl	Stretch, H-bonded	Strong, broad	34.42
3084	=C-H	Alkene	Stretch	Strong	6.88
2924	C-H	Alkane	Stretch, symmetric	Strong	8.82
2858	C-H	Alkane	Stretch, asymmetric	Strong	3.77
2517	O-H	Carb. Acid	Stretch/Broad	Strong	3.63
1943	=C-H	Alkene	Stretch, asymmetric	Strong	1.89
1718	C=O	Carbonyl/Ketone	Stretch	Strong	45.95
1610	C=C	Arom./Arene	Scissoring	Med	43.94
1537	N=O	Nitro Arene	Stretch, asymmetric	Strong	14.74
1450	-C-H	Alkane	Bending	Variable	1.02
1341	N=O	Nitro Arene	Stretch, symmetric	Strong	1.17
1260	C-O/Ar-O-NO_2	Ether/Ester/Covalent Nitrate	Stretch	Med-Weak	122.15
909	=C-H	Alkene	Bending	Strong	0.72
763	O-H/ C=C/N-H	Alcohol/Arene/Amine	Bending, out-of-plane	Weak	6.63

Table 5c

Table 5: FTIR analysis of Mohuda (MH) coal

Likewise, total area of 33.91 cm^2 of -CH_3 group in raw coal at 2917 cm^{-1}, 2856 cm^{-1} and at 1439 cm^{-1} is decreased to 21.47 cm^2 at 2923 cm^{-1}, 2856 cm^{-1} and at 1452 cm^{-1} in GT_G coal (Table 6a & 6b) and total area of CH_3 group is decreased to 13.59 cm^2 at 2923 cm^{-1}, 2859 cm^{-1} and at 1447 cm^{-1} for SMC in aqueous medium (Table 6a & 6c).

GT_D					
Wave Number (cm^{-1})	Functional Group		Type of Vibration	Intensity	Area (cm^2)
3414	O-H	Phenolic/Hydroxyl	Stretch, H-bonded	Strong, broad	2.18
3033	=C-H	Alkene	Stretch	Strong	0.32
2917	C-H	Alkane	Stretch, symmetric	Strong	11.63
2856	C-H	Alkane	Stretch, asymmetric	Strong	8.17
1596	C=C	Arom./Arene	Scissoring	Med	5.43
1439	-C-H	Alkane	Bending	Variable	14.11
1368	N=O/C-H	Nitro/Alkane	Stretch, symmetric	Strong/variable	0.82
1320	C-N	Amine	Stretch	Strong	0.92
1032	C-O	Ether/Ester	Stretch	Strong	0.72
866	=C-H/ C=C/N-H	Alkene/Arene/Amine	Bending	Strong	0.92
808	=C-H/ C=C/N-H	Alkene/Arene/Amine	Bending	Strong	1.36
748	O-H/ C=C/N-H	Alcohol/Arene/Amine	Bending, out-of-plane	Weak	1.99

Table 6a

GT_G					
Wave Number (cm^{-1})	Functional Group		Type of Vibration	Intensity	Area (cm^2)
3432	O-H	Phenolic/Hydroxyl	Stretch, H-bonded	Strong, broad	5.81
3065	=C-H	Alkene	Stretch	Strong	0.44
2923	C-H	Alkane	Stretch, symmetric	Strong	10.34
2856	C-H	Alkane	Stretch, asymmetric	Strong	3.61
1913	C=C	Arom./Arene	Stretch	Strong	1.45
1707	C=O	Carbonyl/Ketone	Stretch	Strong	5.54
1602	C=C	Arom./Arene	Scissoring	Med	13.39
1525	N=O	Nitro Arene	Stretch, asymmetric	Strong	9.24
1452	-C-H	Alkane	Bending	Variable	7.52
1329	N=O	Nitro Arene	Stretch, symmetric	Strong	14.35
1030	C-O	Ether/Ester	Stretch	Strong	9.34
888	=C-H/ C=C/N-H	Alkene/Arene/Amine	Bending	Strong	0.64
820	=C-H/ C=C/N-H	Alkene/Arene/Amine	Bending	Strong	1.22
751	O-H/ C=C/N-H	Alcohol/Arene/Amine	Bending, out-of-plane	Weak	2.43

Table 6b

GT_A					
Wave Number (cm^{-1})	Functional Group		Type of Vibration	Intensity	Area (cm^2)
3437	O-H	Phenolic/Hydroxyl	Stretch, H-bonded	Strong, broad	55.15
3077	=C-H	Alkene	Stretch	Strong	1.24
2923	C-H	Alkane	Stretch, symmetric	Strong	4.50
2859	C-H	Alkane	Stretch, asymmetric	Strong	2.27
2506	O-H	Carb. Acid	Stretch/Broad	Strong	2.29
1934	C=C	Arom./Arene	Stretch	Strong	6.03
1715	C=O	Carbonyl/Ketone	Stretch	Strong	39.29
1606	C=C	Arom./Arene	Scissoring	Med	48.28
1532	N=O	Nitro Arene	Stretch, asymme	Strong	14.19
1447	-C-H	Alkane	Bending	Variable	6.83
1339	N=O	Nitro Arene	Stretch, symmetric	Strong	4.06
1256	C-O/Ar-O-NO_2	Ether/Ester/Covalent Nitrate	Stretch	Med-Weak	122.29
905	=C-H	Alkene	Bending	Strong	0.94
826	=C-H/ C=C/N-H	Alkene/Arene/Amine	Bending	Strong	0.77
759	O-H/ C=C/N-H	Alcohol/Arene/Amine	Bending, out-of-plane	Weak	7.73

Table 6c

Table 6: FTIR analysis of Gasalitand (GT) coal

Total areas of -CH_3 group in demineralized coal at (2917 cm^{-1}, 2854 cm^{-1} and at 1439 cm^{-1}) is 13.91 cm^2 decreased to 13.05 cm^2 in SL_G (2921 cm^{-1}, 2855 cm^{-1} and at 1446 cm^{-1}; Table 7a & 7b) and area of CH_3 group is decreased to 7.54 cm^2 at 2922 cm^{-1}, 2856 cm^{-1} and at 1449 cm^{-1} in SL_A coal (Table 7a & 7c).

SL_D					
Wave Number (cm^{-1})	Functional Group		Type of Vibration	Intensity	Area (cm^2)
3440	O-H	Phenolic/Hydroxyl	Stretch, H-bonded	Strong, broad	0.12
3043	=C-H	Alkene	Stretch	Strong	0.66
2917	C-H	Alkane	Stretch, symmetric	Strong	0.94
2854	C-H	Alkane	Stretch, asymmetric	Strong	0.49
1897	C=C	Arom./Arene	Stretch	Strong	0.45
1594	C=C	Arom./Arene	Scissoring	Med	7.95
1439	-C-H	Alkane	Bending	Variable	12.48
1220	C-O	Ether/Ester	Stretch	Strong	27.44
865	=C-H/ C=C/N-H	Alkene/Arene/Amine	Bending	Strong	1.19
807	=C-H/ C=C/N-H	Alkene/Arene/Amine	Bending	Strong	2.00
748	O-H/ C=C/N-H	Alcohol/Arene/Amine	Bending, out-of-plane	Weak	3.65

Table 7a

SL_G					
Wave Number (cm^{-1})	Functional Group		Type of Vibration	Intensity	Area (cm^2)
3435	O-H	Phenolic/Hydroxyl	Stretch, H-bonded	Strong, broad	7.79
3058	=C-H	Alkene	Stretch	Strong	1.22
2921	C-H	Alkane	Stretch, symmetric	Strong	5.61
2855	C-H	Alkane	Stretch, asymmetric	Strong	2.83
1916	C=C	Arom./Arene	Stretch	Strong	3.78
1703	C=O	Carbonyl/Ketone	Stretch	Strong	8.71
1599	C=C	Arom./Arene	Scissoring	Med	23.07
1524	N=O	Nitro Arene	Stretch, asymmetric	Strong	10.30
1446	-C-H	Alkane	Bending	Variable	4.61
1326	N=O	Nitro Arene	Stretch, symmetric	Strong	88.03
886	=C-H/ C=C/N-H	Alkene/Arene/Amine	Bending	Strong	0.36
820	=C-H/ C=C/N-H	Alkene/Arene/Amine	Bending	Strong	1.30
751	O-H/ C=C/N-H	Alcohol/Arene/Amine	Bending, out-of-plane	Weak	3.06

Table 7b

SL_A					
Wave Number (cm^{-1})	Functional Group		Type of Vibration	Intensity	Area (cm^2)
3422	O-H	Phenolic/Hydroxyl	Stretch, H-bonded	Strong, broad	20.66
2922	C-H	Alkane	Stretch, symmetric	Strong	4.53
2856	C-H	Alkane	Stretch, asymmetric	Strong	1.94
1930	C=C	Arom./Arene	Stretch	Strong	2.21
1711	C=O	Carbonyl/Ketone	Stretch	Strong	9.68
1605	C=C	Arom./Arene	Scissoring	Med	22.15
1528	N=O	Nitro Arene	Stretch, asymmetric	Strong	7.05
1449	-C-H	Alkane	Bending	Variable	1.08
1374	N=O	Nitro Arene	Stretch, symmetric	Strong	0.64
1334	N=O	Nitro Arene	Stretch, symmetric	Strong	2.56
1274	C-O/Ar-O-NO_2	Ether/Ester/Covalent Nitrate	Stretch	Med-Weak	65.66
895	=C-H/ C=C/N-H	Alkene/Arene/Amine	Bending	Strong	0.14
825	=C-H/ C=C/N-H	Alkene/Arene/Amine	Bending	Strong	0.59
754	O-H/ C=C/N-H	Alcohol/Arene/Amine	Bending, out-of-plane	Weak	2.29

Table 7c

Table 7: FTIR analysis of Salanpur (SL) coal

Total areas of CH_3 group in demineralized coal at (2918 cm^{-1}, 2854 cm^{-1} and at 1440 cm^{-1}) is 20.56 cm^2 decreased to 20.13 cm^2 in ST_G (2922 cm^{-1}, 2856 cm^{-1} and at 1452 cm^{-1}; Table 8a & 8b) and total area of -CH_3 group decreased to 19.99 cm^2 in ST_A at 2922 cm^{-1}, 2857 cm^{-1} and at 1447 cm^{-1} (Table 8a & 8c).

ST_D					
Wave Number (cm^{-1})	Functional Group		Type of Vibration	Intensity	Area (cm^2)
3414	O-H	Phenolic/Hydroxyl	Stretch, H-bonded	Strong, broad	5.76
3042	=C-H	Alkene	Stretch	Strong	0.95
2918	C-H	Alkane	Stretch, symmetric	Strong	4.33
2854	C-H	Alkane	Stretch, asymmetric	Strong	1.82
1901	C=C	Arom./Arene	Stretch	Strong	0.47
1599	C=C	Arom./Arene	Scissoring	Med	31.25
1440	-C-H	Alkane	Bending	Variable	14.41
1253	C-O	Ether/Ester	Stretch	Strong	35.60
874	=C-H/ C=C/N-H	Alkene/Arene/Amine	Bending	Strong	1.62
815	=C-H/ C=C/N-H	Alkene/Arene/Amine	Bending	Strong	2.48
753	O-H/ C=C/N-H	Alcohol/Arene/Amine	Bending, out-of-plane	Weak	3.38

Table 8a

ST_G					
Wave Number (cm^{-1})	Functional Group		Type of Vibration	Intensity	Area (cm^2)
3427	O-H	Phenolic/Hydroxyl	Stretch, H-bonded	Strong, broad	17.30
3064	=C-H	Alkene	Stretch	Strong	0.48
2922	C-H	Alkane	Stretch, symmetric	Strong	9.57
2856	C-H	Alkane	Stretch, asymmetric	Strong	3.98
1922	C=C	Arom./Arene	Stretch	Strong	0.01
1708	C=O	Carbonyl/Ketone	Stretch	Strong	10.02
1603	C=C	Arom./Arene	Scissoring	Med	28.04
1527	N=O	Nitro Arene	Stretch, asymmetric	Strong	8.76
1452	-C-H	Alkane	Bending	Variable	6.58
1374	N=O	Nitro Arene	Stretch, symmetric	Strong	32.10
1333	N=O	Nitro Arene	Stretch, symmetric	Strong	54.10
894	=C-H/ C=C/N-H	Alkene/Arene/Amine	Bending	Strong	0.44
826	=C-H/ C=C/N-H	Alkene/Arene/Amine	Bending	Strong	1.32
757	O-H/ C=C/N-H	Alcohol/Arene/Amine	Bending, out-of-plane	Weak	1.96

Table 8b

ST_A					
Wave Number (cm^{-1})	Functional Group		Type of Vibration	Intensity	Area (cm^2)
3440	O-H	Phenolic/Hydroxyl	Stretch, H-bonded	Strong, broad	68.34
3077	=C-H	Alkene	Stretch	Strong	2.22
2922	C-H	Alkane	Stretch, symmetric	Strong	5.85
2857	=C-H	Alkane	Stretch, asymmetric	Strong	2.70
2516	O-H	Carb. Acid	Stretch/Broad	Strong	2.27
1941	=C-H	Alkene	Stretch, asymmetric	Strong	2.19
1717	C=O	Carbonyl/Ketone	Stretch	Strong	46.74
1607	C=C	Arom./Arene	Scissoring	Med	48.12
1533	N=O	Nitro Arene	Stretch, asymmetric	Strong	11.75
1447	-C-H	Alkane	Bending	Variable	11.44
1340	N=O	Nitro Arene	Stretch, symmetric	Strong	5.24
1264	C-O/Ar-O-NO_2	Ether/Ester/Covalent Nitrate	Stretch	Med-Weak	113.27
908	=C-H	Alkene	Bending	Strong	2.12
831	=C-H/ C=C/N-H	Alkene/Arene/Amine	Bending	Strong	2.34
763	O-H/ C=C/N-H	Alcohol/Arene/Amine	Bending, out-of-plane	Weak	8.49

Table 8c

Table 8: FTIR analysis of Shatabdi (ST) coal

This is a very significant finding that the decrease in total areas of alkane groups of demineralized and treated coals suggests the replacement of aliphatic side chains by nitro group.

4.0 Conclusion

The variation of molecular structure of selected coals of Jharia Basin of Indian and their modifications through nitric acid treatment in acetic acid and aqueous media shows that the changes in the structural parameters and the aromaticity of the treated coals are dependent upon coal rank and the medium of treatment. Nitration has

increased weight of SMCs in non-aqueous medium for all the coals under the present study. Whereas, the nitration in aqueous medium shows loss in weight for Mohuda (MH) coal and gain in weight for higher rank coals. Nitration in aqueous medium occurs simultaneous with oxidation of the coal matrix which removes more aliphatic side chains in the coal moieties, resulting relative increase in weight than that of non-aqueous medium. Significant observation in the present study is that nitration in both the media is capable of removing the aliphatic side chains for the coals and aromaticity increases with increase in rank (vitrinite reflectance) of coal.

FTIR studies show that coal arenes of the raw coals are converted into nitro-arenes in SMCs, the corresponding bands at 1550–1490 cm^{-1} and 1355–1315 cm^{-1} respectively. In the case of low rank coals, glacial acetic acid medium being milder medium might have resulted in the formation of covalent nitro groups (Ar–O–NO_2) in the range 1300–1255 cm^{-1} which is absent in relatively stronger aqueous medium where oxidation is also active phenomenon. FTIR study of nitric acid coals treated in both the media show introduction of nitrogen (-N) and oxygen (-O) containing groups and newly formed aromatic nucleus different from the raw coals which confirms the formation of structurally modified coals (SMCs). The areas under each functional group for demineralized samples and their corresponding SMCs have been calculated. The results show that the content of alkane group is decreased in SMCs corresponding to aliphatic and alicyclic (-CH) functional group of vibration (2950–2800 cm^{-1}) and bending vibration of alkane (-CH; 1470–1350 cm^{-1}). The decrease in total areas of alkane group in treated coals than that of raw coals suggests the replacement of aliphatic side chains by nitro group.

The present study also reveals that in the SMCs of coals namely GT, SL and ST shows a considerable increase in aromaticity in aqueous medium and these are candidate coals for manufacturing of specialty carbon materials such as fullerene, artificial graphite, activated carbon and artificial diamond.

Declarations

ACKNOWLEDGEMENTS:

We thank the Director, CSIR-Central Institute of Mining and Fuel Research, Dhanbad for permission to publish this paper. We also thank our colleagues at the Resource Quality Assessment and CTL Research Group for their support.

Availability of data and materials:

All data have been provided

Competing interests:

Not Applicable

Funding:

No funding to be mentioned

Authors' contributions:

This is a PhD work of the First Author under the guidance of the Other two authors

References

1. ASTM D5016 (2016) Standard test method for total sulfur in coal and coke combustion residues using a high-temperature tube furnace combustion method with infrared absorption
2. ASTM D5373 (2016) Standard test methods for determination of carbon, hydrogen and nitrogen in analysis samples of coal and carbon in analysis samples of coal and coke
3. ASTM D5865 (2013) Standard test method for gross calorific value of coal and coke
4. Barbara K, Slawomira P, Brett JV, ICCP (2019) Application of electron microscopy TEM and SEM for analysis of coals, organic rich shales and carbonaceous matter. Int J Coal Geol 211:1–13. https://doi.org/10.1016/j.coal.2019.05.010
5. Baysal M, Yürüm A, Yildiz B, Yürüm Y (2016) Structure of some western Anatolia coals investigated by FTIR, Raman, ^{13}C solid state NMR spectroscopy and X-ray diffraction. Int J Coal Geol 163:166–176. https://doi.org/10.1016/j.coal.2016.07.009
6. Boral P, Varma AK, Maity S (2015) X-ray diffraction studies of some structurally modified Indian coals and their correlation with petrographic parameters. Curr Sci 108(3):384–394
7. Borrego AG, Marbán G, Alonso MJG, Älvarez D, Menéndez R (2000) Maceral effects in the determination of proximate volatiles in coals. Energy Fuels 14:117–126. https://doi.org/10.1021/ef990050t
8. Chandra D (1992) Jharia Coalfield. Geological Society of India, India
9. Dangyu S, Cunbei Y, Xiaokui Z, Xianbo S, Xiaodong Z (2011) Structure of the organic crystalline unit in coal as determined by X-ray diffraction. Mining Science Technology (China) 21:667–671. http://dx.doi.org/10.1016/j.mstc.2011.10.004
10. Domazetis G, James BD (2006) Molecular models of brown coal containing inorganic species. Org Geochem 37:244–259. doi:10.1016/j.orggeochem.2005.07.006
11. Guerrero A, Diez MA, Borrego AG (2013) Effect of volatile matter release on optical properties of macerals from different rank coals. Fuel 114:21–30. https://doi.org/10.1016/j.fuel.2012.05.023
12. Hirsch PB (1954) X-Ray scattering from coals. Proceedings of the Royal Society (London) A 226:143–169
13. IS 436 Part 1/Sec 1 (2001) Methods of sampling of coal and coke, Part 1: Sampling of coal, Sect. 1: Manual sampling
14. IS 9127 Part 2 (2002) Methods for the petrographic analysis of bituminous coal and anthracite — Part 2: Method of preparing coal samples
15. IS 9127 Part 3 (2002) Methods for the petrographic analysis of bituminous coal and anthracite — Part 3: Method of determining maceral group composition
16. IS 9127 Part 5 (2004) Methods for the petrographic analysis of bituminous coal and anthracite —Part 5: Method of determining microscopically the reflectance of vitrinite
17. Krishnan MS (1982) Geology of India and Burma. C.B.S. Publishers and Distributors, India
18. Li K, Khanna R, Zhang J, Barati M, Liu Z, Xu T, Yang T, Sahajwalla V (2015) Comprehensive investigation of structural features of bituminous coals using advanced analytical techniques. Energy Fuels 29:7178–7189. https://doi.org/10.1021/acs.energyfuels.5b02064

19. Lu L, Sahajwalla V, Kong C, Harris D (2001) Quantitative X-ray diffraction analysis and its application to various coals. Carbon 39(00):1821–1833. https://doi.org/10.1016/S0008-6223 00318–3
20. Maity S, Choudhury A (2008) Influence of nitric acid treatment in different media on X-ray structural parameters of coal. Energy Fuels 22:4087–4091. https://doi.org/10.1021/ef800424w
21. Maity S, Mukherjee P (2006) X-ray structural parameters of some Indian coals. Curr Sci 91:337–340
22. Manoj B, Kunjomana AG (2012) Study of stacking structure of amorphous carbon by X-ray diffraction technique. Int J Electrochem Sci 7:3127–3134
23. Mathews JP, Chaffee AL (2012) The molecular representations of coal – A review. Fuel 96:1–14. http://dx.doi.org/10.1016/j.fuel.2011.11.025
24. Painter PC, Coleman MM (1979) Application of Fourier-transform infrared spectroscopy to the characterization of fractionated coal liquids. Fuel 58(79):301–308. https://doi.org/10.1016/0016-2361 90141–8
25. Painter PC, Coleman MM, Jenkins RG, Walker PL Jr (1978) Fourier transform infrared study of acid-demineralized coal. Fuel 57:125–126. https://doi.org/10.1016/0016-2361(78)90113-8
26. Solomon PR, Serio MA, Carangelo RM, Bassilakis R, Gravel D, Baillargeon M, Baudais F, Vail G (1990) Analysis of the Argonne premium coal samples by thermogravimetric Fourier transform infrared spectroscopy. Energy Fuels 4:319–333. https://doi.org/10.1021/ef00021a017
27. Solum MS, Pugmire RJ, Grant DM (1989) Carbon-13 solid-state NMR of Argonne premium coals. Energy Fuels 3:187–193. https://doi.org/10.1021/ef00014a012
28. Sonibare OO, Haeger T, Foley SF (2010) Structural characterization of Nigerian coals by X-ray diffraction, Raman and FTIR spectroscopy. Energy 35:5347–5353. http://dx.doi.org/10.1016/j.energy.2010.07.025
29. Takagi H, Maruyama K, Yoshizawa N, Yamada Y, Sato Y (2004) XRD analysis of carbon stacking structure in coal during heat treatment. Fuel 83:2427–2433. https://doi.org/10.1016/j.fuel.2004.06.019
30. Tamarkina YV, Shendrik TG, Krzton A, Kucherenko VA (2002) Reactivity and structural modification of coals in HNO_3–Ac_2O system. Fuel Proc Tech 77–78:9–15. https://doi.org/10.1016/S0378-3820 (02)00059 – 0
31. Wertz DL, Bissell M (1994) Relating the non ideal diffraction from the graphene layer stacking peak to the aliphatic carbon abundance in bituminous coals. Energy Fuels 8:613–617. https://doi.org/10.1021/ef00045a016
32. Wertz DL, Bissell M (1995) One-dimensional description of the average polycyclic aromatic unit in Pocahontas No. 3 coal: an X-ray scattering study. Fuel 74:1431–1435. https://doi.org/10.1016/0016-2361 (95)00107-G
33. Wertz DL (1998) X-ray scattering analysis of the average poly-cyclic aromatic unit in Argonne premium coal 401. Fuel 77:43–53. https://doi.org/10.1016/S0016-2361(97)00150-6
34. Wertz DL, Quin JL (2000) Wide angle X-ray scattering study of the layering in three of the Argonne premium coals. Fuel 79:1981–1989. https://doi.org/10.1016/S0016-236 (00)00026 – 0

Figures

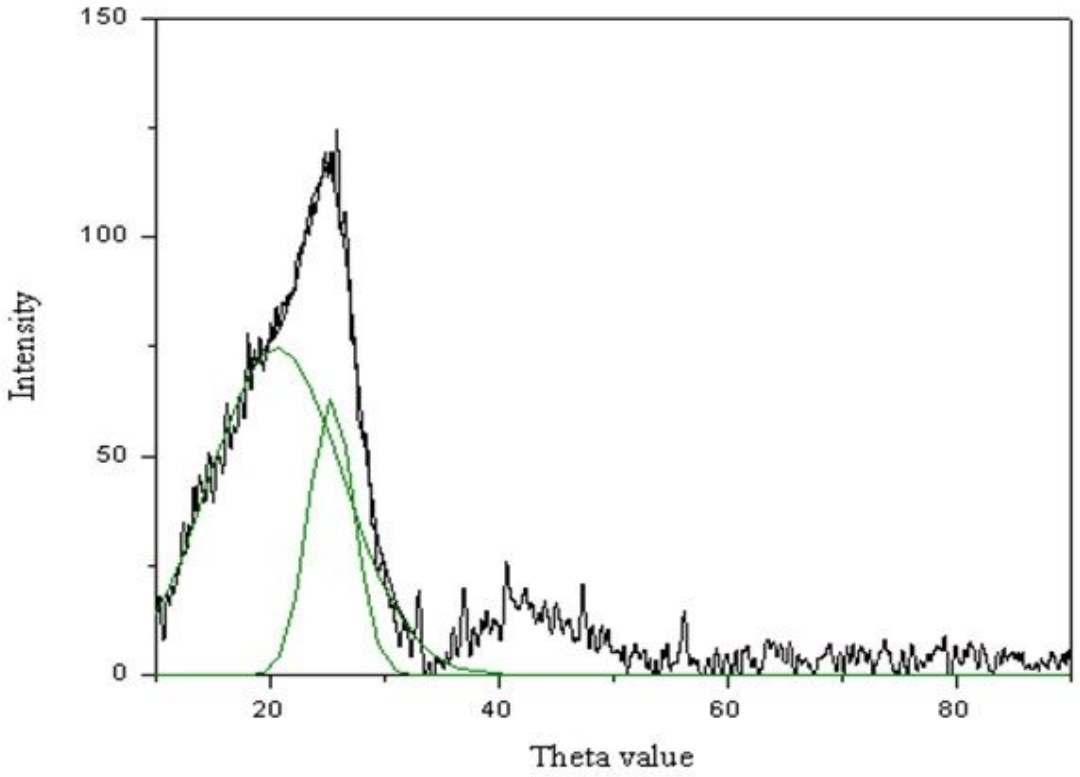

Figure 1

XRD profile curve fitting of two Gaussian peaks for the Mohuda (MH) demineralized coal in the range of 10–35°.

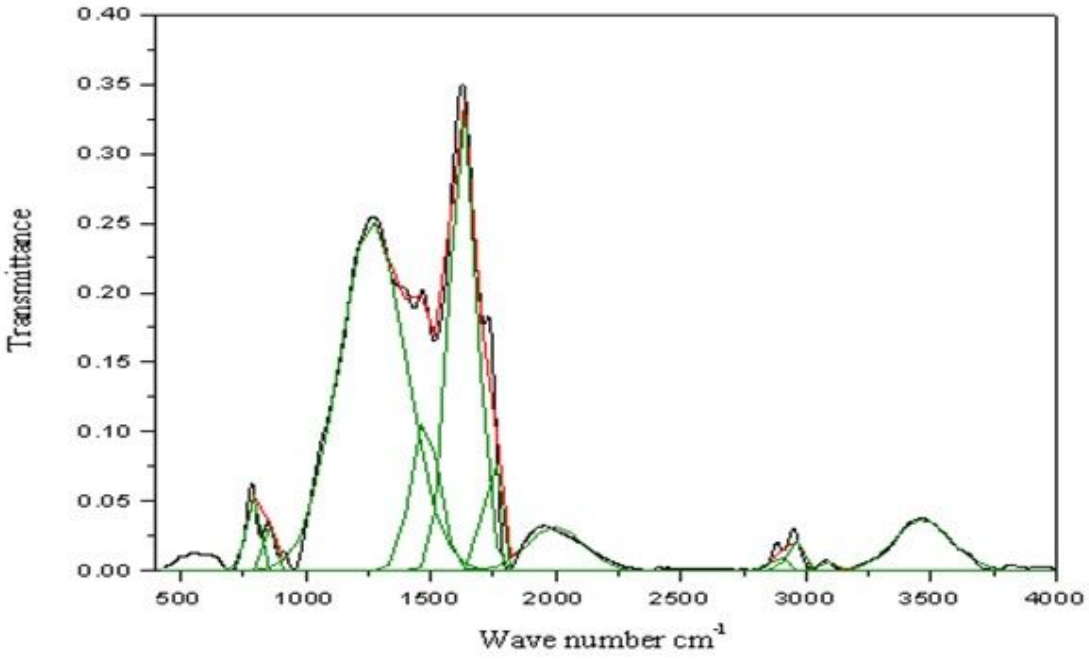

Figure 2

Multi-peak Gaussian probability curve fit of FTIR analysis of Mohuda (MH)

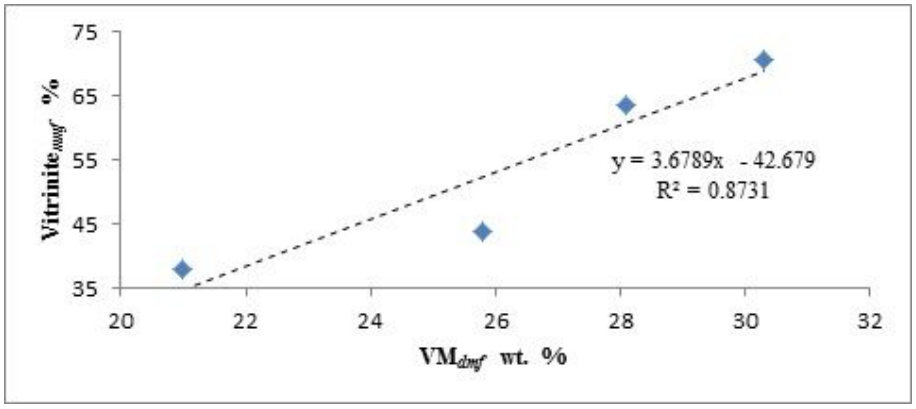

Figure 3

Relation of Vitrinite content with respect to Volatile Matter.

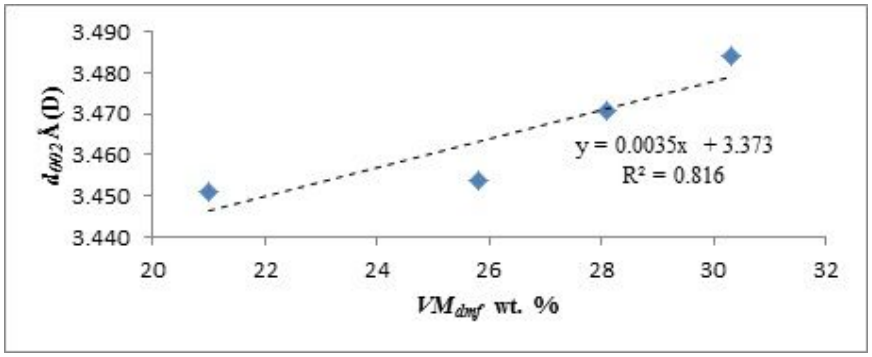

Figure 4

Relation of d002 with respect to Volatile Matter.

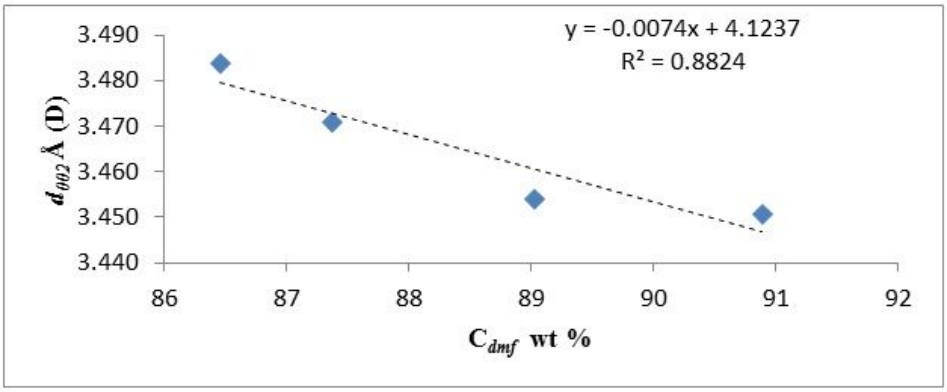

Fig: 5 a

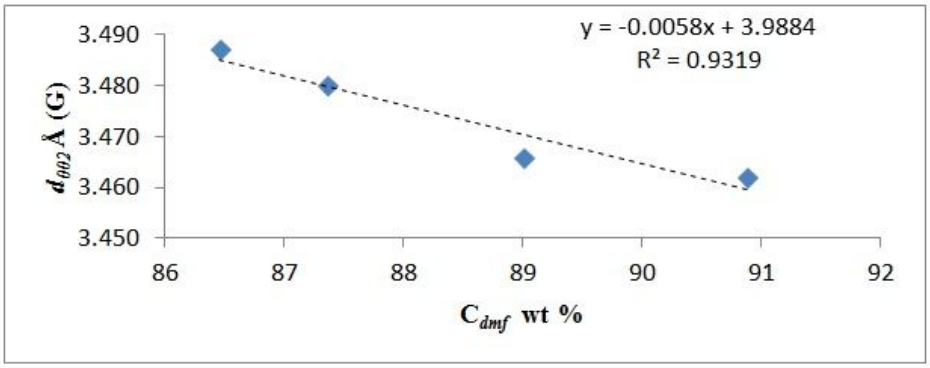

Fig: 5b

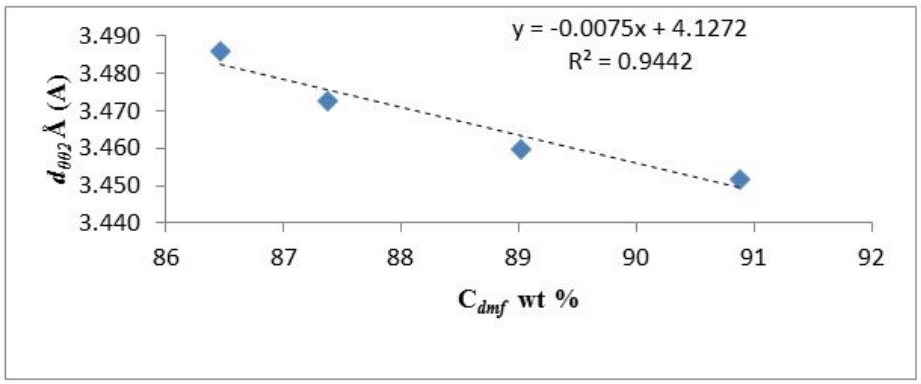

Fig: 5c

Figure 5

a – 5c: Relation of d002 with respect to Cdmf. a) demineralized [(d002 (D)], b) nitration in glacial acetic acid medium [(d002 (G)], c) nitration in aqueous medium [(d002(A)] coals respectively.

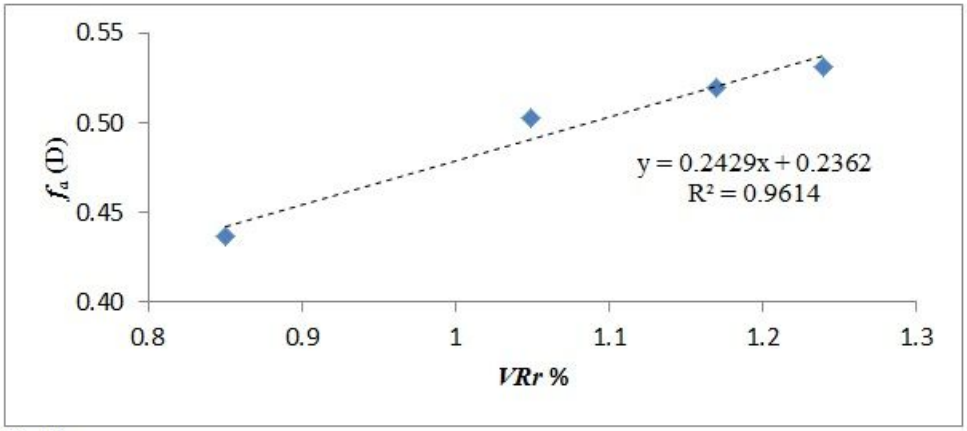

Fig6 a

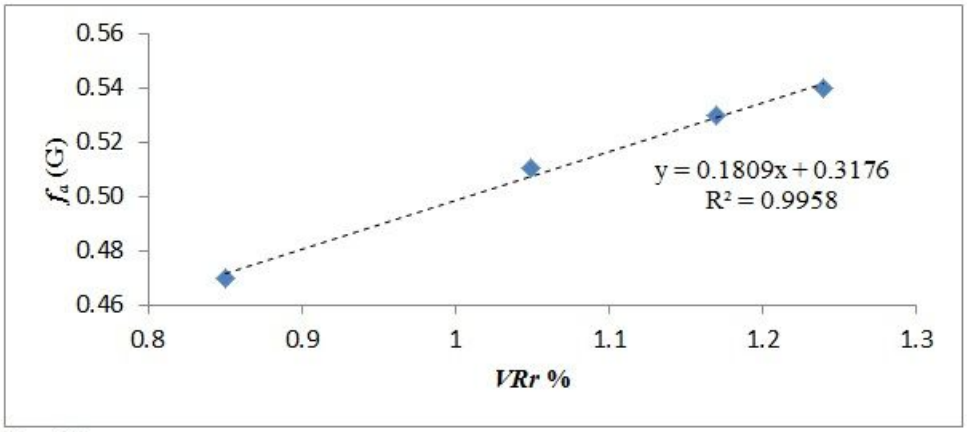

Fig. 6b

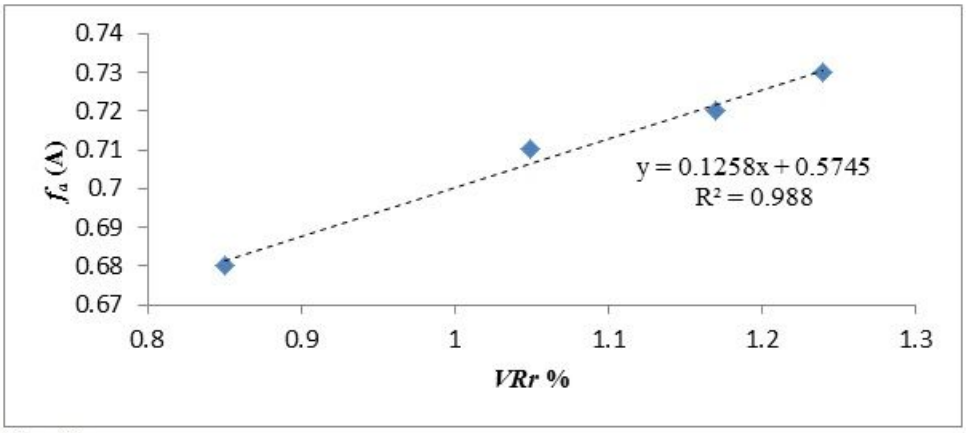

Fig. 6c

Figure 6

a – 6c: Relation of fa with respect to VRr %. a) demineralized [(fa (D)], b) nitration in glacial acetic acid medium [(fa (G)] and c) nitration in aqueous medium [(fa (A)] coals respectively.

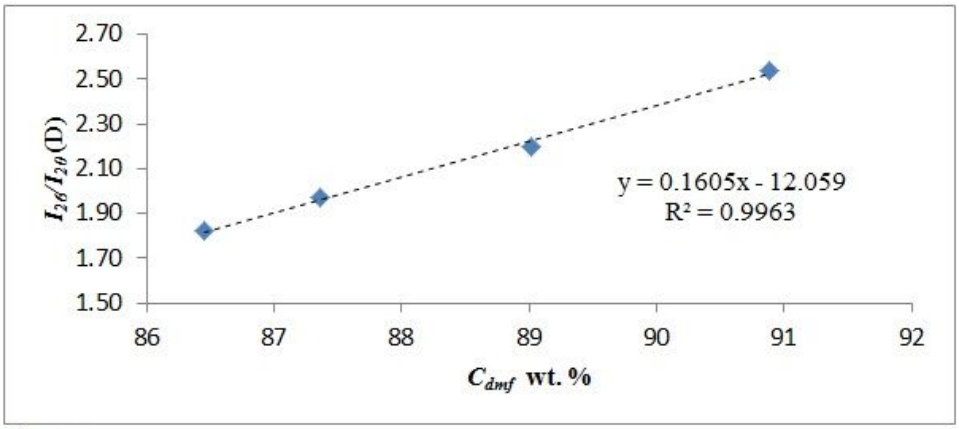

Fig. 7a

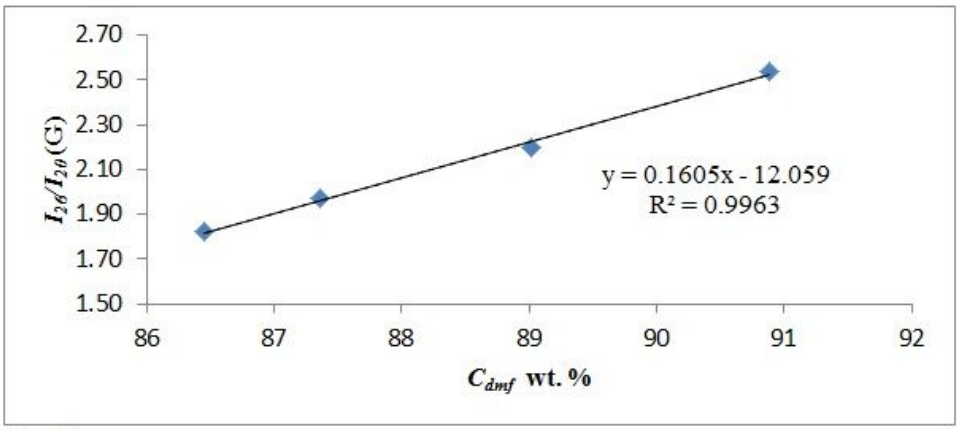

Fig. 7b

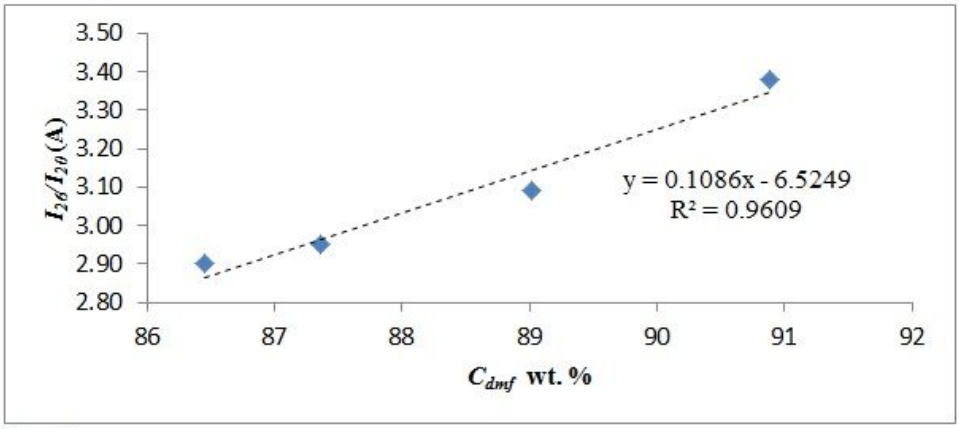

Fig. 7c

Figure 7

a – 7c: Relation of I26/I20 with respect to Cdmf. a) demineralized [(I26/I20 (D)], b) nitration in glacial acetic acid medium [(I26/I20 (G)] and c) nitration in aqueous medium [(I26/I20 (A)] coals respectively.

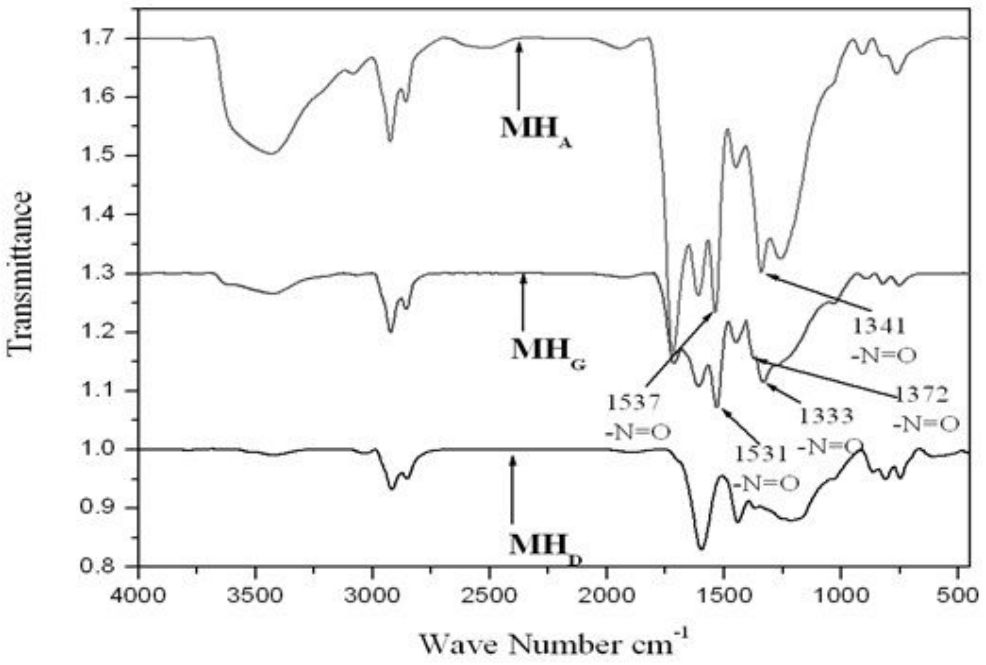

Figure 8

FTIR curves of Mohuda (MH) coal.

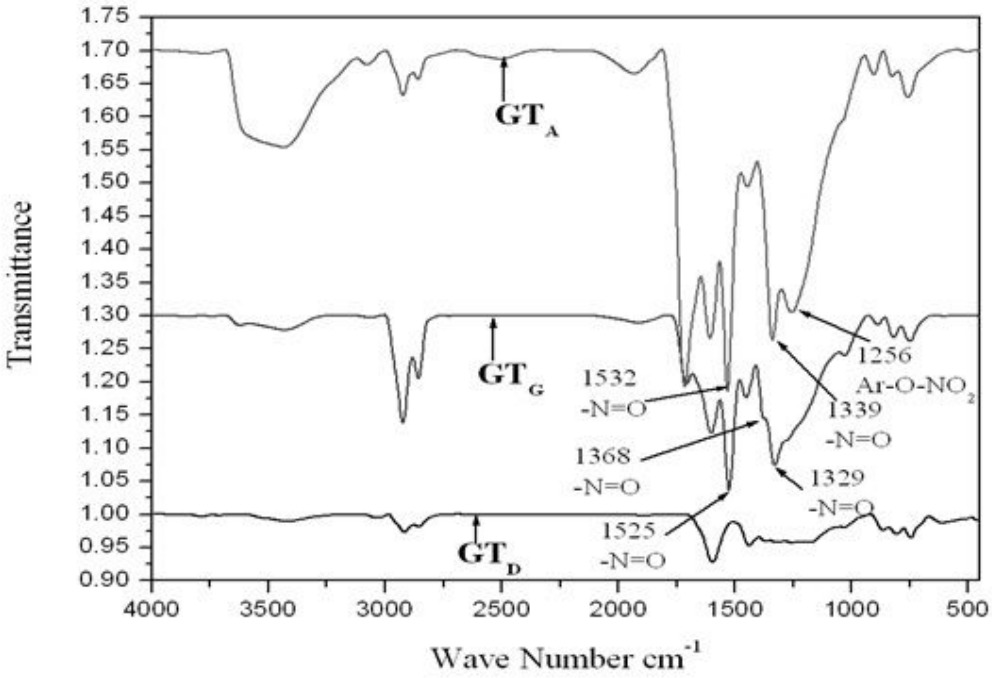

Figure 9

FTIR curves of Gasalitand (GT) coal.

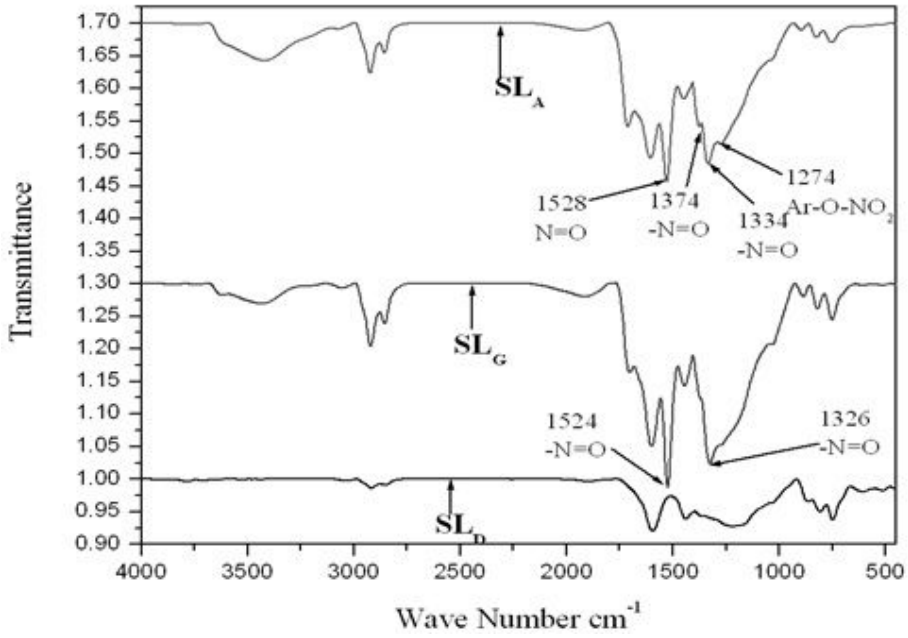

Figure 10

FTIR curves of Salanpur (SL) coal.

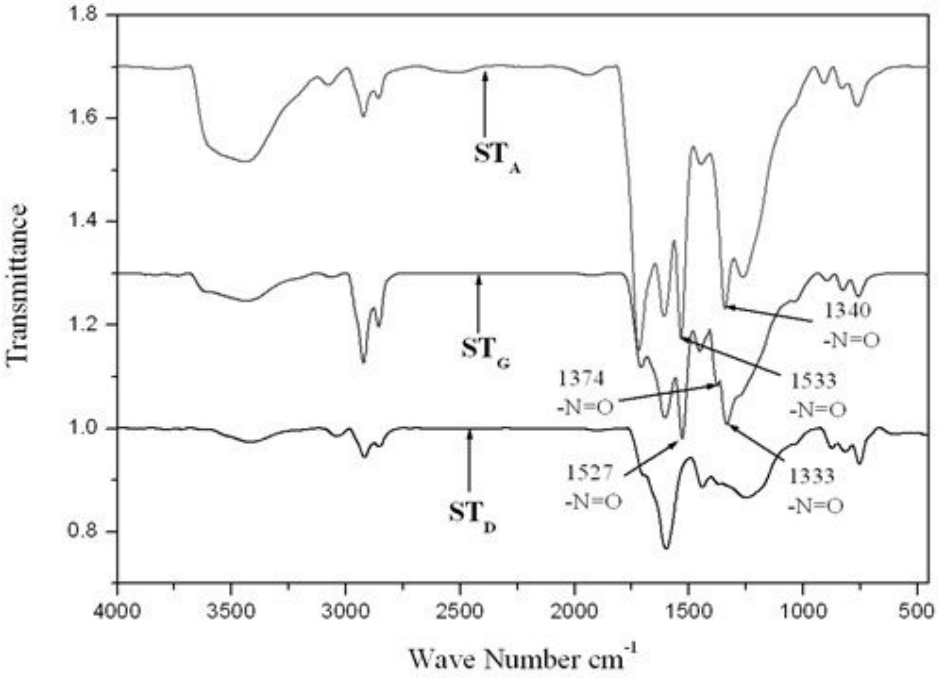

Figure 11

FTIR curves of Shatabdi (ST) coal